Cavendish Laboratory
Surface Physics Group

UNIVERSITY OF CAMBRIDGE

SURFACE NANOSCIENCE SCHOOL 2020

# Fast Motion, the Initial Drop and the Onset of Friction

June 22nd 2020
August 28th 2020

Kit Gallagher

The motion line-shape in the intermediate scattering function, particularly in the ballistic region, is considered for the Li/ Cu (111) system. The effect of varying environmental parameters is demonstrated on particle trajectories, and the resulting ISFs were in agreement with the analytic lineshapes. When fitting the ballistic ISF to a general Gaussian, the wavevector K and the inverse of the standard deviation $\sigma$ are shown to be directly proportional, in agreement with 2D ideal gas law. While traditional analysis methods rely on the central limit theorem, so the experimental noise spectrum need not be consistent with that used in Langevin simulations, a coloured noise approach is used here to better replicate the physical impulse spectrum experienced by the adatoms. In conjunction with a potential energy surface, this is used to produce simulations in wider agreement with existing experimental measurements of this system, into the short-time ballistic region.

## 1 Introduction

Helium-3 surface spin echo (HeSE) is an inelastic scattering technique in surface science that has been used to measure microscopic dynamics at well-defined surfaces in ultra-high vacuum [1]. The information available from HeSE complements and extends that available from other inelastic scattering techniques, and is particularly appropriate for measuring adsorbate dynamics at surfaces, as it provides surface correlation measurements in the picosecond to nanosecond time range [2].

While such surface dynamics can be modelled through the popular Monte Carlo approach, this is costly and inefficient. An alternative is to use Langevin equation based molecular dynamics (MD) simulations [3], where the interaction of adsorbates with the substrate atoms is described using a frozen potential energy surface (PES), a drag term and a stochastic fluctuating force.

The effect of coloured noise on particle trajectories is described by the Generalised Langevin Equation (GLE) in Section 2.3. This is modelled using the PIGLE software [4], described in section 3.1, and contrasted to experimental data of Li on a Cu(111) surface from X. All simulations at baseline parameters $m = 7amu, T = 140K, \eta = 5ps^{-1}$, with no inter-particle interactions, unless otherwise stated.

## 2 Theoretical Background

The observable quantity in the spin-echo experiment is the Intermediate Scattering Function (ISF), which is the autocorrelation of the time-dependent amplitude, A(t).

### 2.1 Langevin Equation

Before consideration of the GLE, it is instructive to first consider the Langevin Equation (LE) which is commonly used to describe surface diffusion. The original Langevin Equation can be extended through consideration of an external (position dependant) potential $V$ and an inter-particle interaction force $\mathbf{F}_{ij}$ between adatoms $i$ and $j$ to give:

$$m\frac{d\mathbf{v}_i}{dt} = -\nabla V - m\lambda\mathbf{v}_i + \boldsymbol{\xi}(t) + \Sigma_{j\neq i}\mathbf{F}_{ij} \tag{1}$$

The stochastic force $\boldsymbol{\xi}(t)$ follows a Gaussian probability distribution with zero mean and the correlation function:

$$\langle \xi_i(t)\xi_j(t')\rangle = 2m\lambda k_B T\delta_{i,j}\delta(t-t') \tag{2}$$

where $k_B$ is Boltzmann's constant, $T$ is the temperature, and $\eta_i$ is the i-th component of the vector $\boldsymbol{\eta}$.

### 2.2 LE Intermediate Scattering Function

While the ISF is defined from the scattering amplitude, it can also be determined directly from the particle's trajectory [5]:

$$I(\mathbf{K},t) = \langle e^{-i\mathbf{K}[\mathbf{R}(t)-\mathbf{R}(0)]}\rangle = \langle e^{-i\mathbf{K}\int_0^t v_{\mathbf{K}}(t')dt'}\rangle \tag{3}$$

where $v_{\mathbf{K}}$ is the velocity of the adparticle projected along the direction of the wavevector $\mathbf{K}$. If a stochastic process is Gaussian and Markovian, Doob's theorem [6] states that its correlation function decays in time exponentially, meaning that the intermediate scattering function can be expressed as:

$$I(\mathbf{K},t) = exp\left[-\chi^2\left(e^{-\frac{t}{\tau_c}} + \frac{t}{\tau_c} - 1\right)\right] \tag{4}$$

where

$$\chi = \tau_c\sqrt{\langle v_{\mathbf{K}}^2\rangle}|\mathbf{K}| = \frac{D|\mathbf{K}|}{\sqrt{\langle v_{\mathbf{K}}^2\rangle}} = \bar{l}|\mathbf{K}| \tag{5}$$

in which $D$ is the diffusion coefficient, and $\bar{l}$ is the mean free path. Note that, in the short time limit $t < \tau_c$, we may approximate the ISF to have a Gaussian form:

$$I(\mathbf{K},t) \propto e^{\frac{-D|\mathbf{K}|^2t^2}{2\tau_c}} \tag{6}$$

### 2.3 Generalised Langevin Equation

However, at short time scales, the LE breaks down as the stochastic force can no longer be considered random so the auto correlation of the stochastic force is no longer zero.

The GLE (given below) combines friction and stochastic terms, and is used to describe this non-Markovian processes, where a complete history of a particles motion is required to predict future motion analytically.

$$m\frac{d\mathbf{v}_i}{dt} = -\nabla V - m\int_{-\infty}^{t} \lambda(t-t')\mathbf{v}_i(t')dt' + \boldsymbol{\zeta}(t) + \Sigma_{j\neq i}\mathbf{F}_{ij} \tag{7}$$

Damping in the form of the memory function $\lambda(t-t')$ and the fluctuating force $\boldsymbol{\zeta}(t)$ are related by the second Fluctuation-Dissipation theorem [7]:

$$\langle \zeta_i(t)\zeta_j(t')\rangle = 2mk_BT\delta_{i,j}\lambda(t-t') \tag{8}$$

### 2.4 GLE Intermediate Scattering Function

It is also possible to consider an analytic form for the ISF in the case of the GLE. This is derived by Townsend et al. [8], and only their results will be replicated here.

The closed form is written as $I(\Delta K,t) = exp[-\Delta K^2 X(t)]$, where $X(t)$ is given by:

$$X(t) = \frac{k_BT}{m\lambda^2}\left(\frac{\lambda}{\omega_c} - 1 + \lambda t + \frac{e^{-\omega_c t/2}}{\omega_c}[C\cosh\omega t + S\sinh\omega t]\right) \tag{9}$$

with the coefficients S and C given by:

$$C = \omega_c - \lambda, \qquad S = \frac{\sqrt{\omega_c}(\omega_c - 3\lambda)}{\sqrt{\omega_c - 4\lambda}} \tag{10}$$

and the frequency scale $\omega$ combines the two basic frequency scales of the problem, $\omega_c$ and $\lambda$, by:

$$\omega = \frac{1}{2}\sqrt{\omega_c^2 - 4\lambda\omega_c} \tag{11}$$

### 2.5 Noise Filters

The primary filter used in this project was a low-pass noise filter. This gives an exponential decay in the memory kernel, which can be represented by the noise source spectral power density. This decay is characterised by the decay time $\tau$ (where $\gamma$ denotes friction), so that $\lambda$ may be written as:

$$\lambda(t) = \frac{\gamma}{\tau}e^{-|t|/\tau}, \qquad \lambda(\omega) = \sqrt{\frac{2}{\pi}}\frac{\gamma}{1+(\tau\omega)^2} \tag{12}$$

## 3 Computational Methodology

### 3.1 PIGLE Software

PIGLE (Particles Interacting in Generalized Langevin Equation) [9] is software used to simulate the dynamics of multi species interacting particles on a periodic energy surface, obeying to the generalized Langevin Equation. The code is based in MATLAB, but uses the Simulink framework to optimise running efficiency.

### 3.2 Program Structure

Initially, the particles are assigned an arbitrary velocity from a thermal distribution corresponding to the simulation temperature, and randomly positioned about the simulation supercell. However, when a non-zero potential is applied, the random initial position of the particle may be unphysical (such as corresponding to a higher energy than the initial thermal distribution, so 'thermalisation time' is included to allow dissipation of this excess energy through friction.

Within the simulation, there are two separate regimes separated by the friction time. On time scales smaller than this characteristic time, the particle moves ballistically as a result of the atomic collisions, whereas on longer time scales the net motion of the particle is diffusive. These two regions can both be observed in the ISF, with the steeper ballistic section commonly being referred to as the 'initial drop'.

## 4 Results

### 4.1 Trajectory Characteristics

On a zero potential surface, the particle undergoes a distinctive random walk trajectory with the displacement scaling in magnitude with temperature, in agreement with the classical temperature dependence of the diffusion coefficient. Furthermore, an increase in the atomic friction coefficient reduces the particle displacement under diffusion, and increases the random noise in the trajectory.

A low-pass filter may be applied to the white noise source, to remove the higher frequency components. The effect of this is clearly visualised in the trajectories in Figure 1, where the higher frequency components of motion are 'smoothed out' as the value of $\tau$ (corresponding to the cut-off frequency of the filter) is increased.

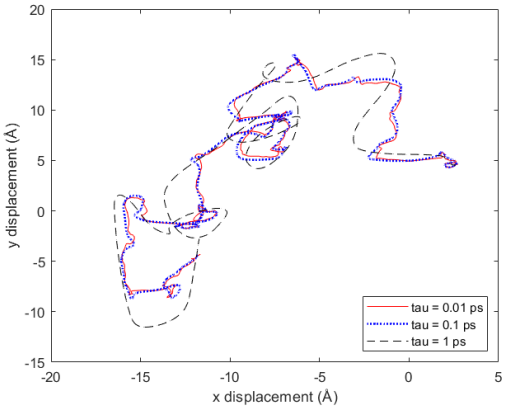


**Fig. 1** The trajectory of a Li particle on a zero potential surface, over 100ps. Note the removal of high frequency aspects to the trajectory when the cut-off time $\tau$ is increased.

An external potential may separately be applied to replicate the atomic surface, giving the trajectory observed in Figure 2. This shows the distinctive 'jump diffusion', whereby a particle's primary motion across a surface is characterised by discrete 'jumps' between potential minima. The scaling of the random walk is reduced, suggesting the particle is primarily confined to areas of lower potential and moves less freely.

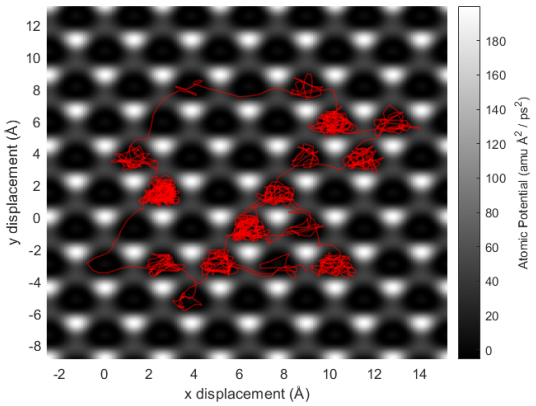


**Fig. 2** The trajectory of a Li particle on a FCC surface, over 100ps at 200K. The darker regions correspond to lower potential, and the lighter regions to higher potential, which the particle trajectory is depicted in red

### 4.2 ISF Characteristics

The ISF is used to characterise the temporal auto-correlation function over time, and is simulated here for comparison with experimental results from Helium spin echo spectroscopy.

Loss of coherence occurs faster when temperature is raised, but slower when friction is increased, due to the relative changes in particle mobility. The addition of a potential surface reduces the decay rate of the ISF, as particles tend to be confined to potential minima on the surface, and so remain correlated for for greater lengths of time.

We may also consider the more general effect of a noise filter on the ISF, as depicted in Figure 3. The characteristic form of the ISF is similar, however the decay occurs faster when a noise filter is applied, in accordance with the analytic solutions to the LE and GLE respectively. This may be attributed to the removal of small, high frequency fluctuations, so the particle is more likely to continue along a constant line of motion away from its initial point, reducing its temporal autocorrelation function.

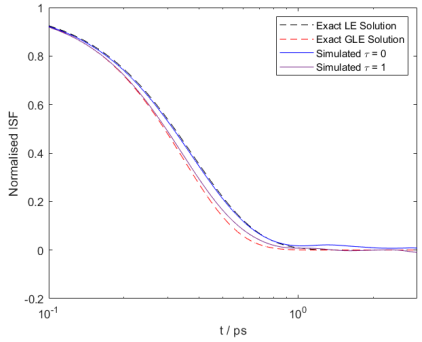


**Fig. 3** The incoherent ISF for a single Li particle on a zero potential surface, averaged over 100 particles, with and without a low-pass noise filter applied (characterised by cut-off time $\tau$). Simulated with parameters $m = 7amu, T = 140K, \eta = 5ps^{-1}, \Delta K = 1\text{Å}^{-1}$, with each ISF normalised separately.

### 4.3 Ballistic and Diffusive Regions

As described in Section 3.2, there are two characteristic regimes; the short time (ballistic) regime and the long time (diffusive) regime. The exact solution for the ISF (4) suggests a short time approximation of a Gaussian form, (6), so in the ballistic region the ISF is fitted to a general Gaussian of the form:

$$I(\mathbf{K},t) = Ae^{-\frac{t^2}{2\sigma^2}} \tag{13}$$

where $A$ and $\sigma$ are fitting parameters. This linear relationship between $\mathbf{K}$ and $1/\sigma$ is characteristic of a gas of quantum particles undergoing ballistic motion [10].

The constant of proportionality is given by $\sqrt{\langle v_{\mathbf{K}}^2 \rangle} = \sqrt{k_B T/m}$ according to (5). This has a theoretical value of 4.078Å, in agreement with the statistical gradient of $4.058 \pm 0.03$Å.

### 4.4 Introduction of a Potential

The main focus of this report is to combine the noise spectrum analysis with a potential surface (depicted in Figure 4), utilising the potential of the PIGLE software. The maxima in energy was taken as $45eV$, corresponding to the height of the top site. The activation energy of diffusion across the saddle point is given as $9eV$, while the intermediate slope energies were set at $13eV$.

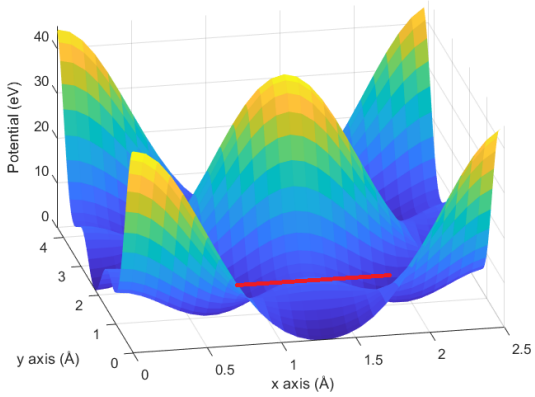


**Fig. 4** The potential energy surface for Cu (111), given over a single unit cell of dimensions $2.56\text{Å} \times 4.43\text{Å}$. The line in red demonstrates the path across the saddle point, which is the preferred route for diffusion.

### 4.5 Experimental Fitting

With the use of the potential energy surface (PES) developed in Section 4.4, we may reproduce plots of fitting parameter $\alpha$ against $\Delta K$ in comparison with experimental data obtained by Ward [11].

Initially the friction and PES were optimised to match the long time diffusive motion of the particle, fitted to a single exponential decay with a background constant (Figure 5a).

An atomic friction coefficient of $1ps^{-1}$ to achieve this fit with the simulated values in the diffusive region. A low-pass noise filter was subsequently added, with the cut-off parameter $\tau$ to be optimised for agreement with the experimental data in the ballistic region, given in Figure 5b.

To consider this faster ballistic decay, the fitted primary exponential decay curves are subtracted from the simulated ISF data.

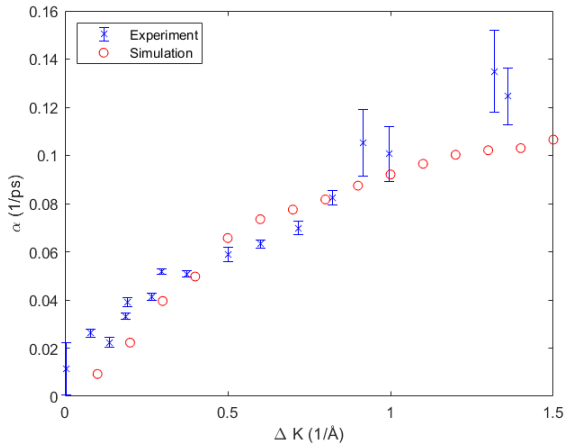


**(a)** Primary Exponential Decay

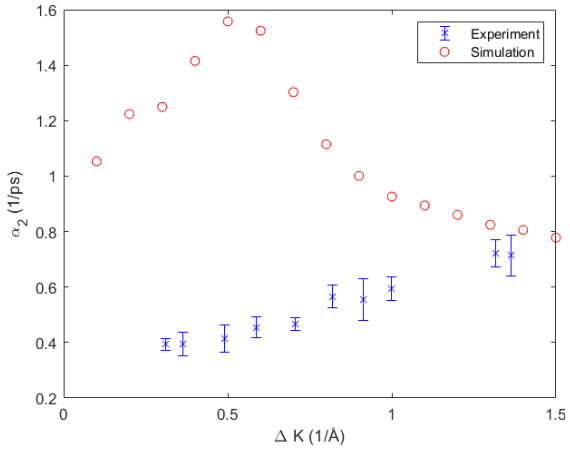


**(b)** Faster Ballistic Decay

**Fig. 5** Fitting parameters $\alpha$ and $\alpha_2$ plotted over $\Delta\mathbf{K}$ for a single particle ISF (over $800ps$, sampled at $10fs$ intervals), with a Cu (111) potential and averaged over 25 particles. All simulations at baseline parameters $m = 7amu, T = 140K, \eta = 1ps^{-1}$, with a set seed for reproducibility.

The residual ISF is then fitted to the equation:

$$I(\mathbf{K},t) = Ce^{-\alpha_2 t} + De^{-\frac{t^2}{2\sigma^2}} \tag{14}$$

where $\alpha_2$ characterises the faster ballistic exponential decay. The primary exponential fit is approached iteratively, ensuring a good fit at longer time scales before increasing the time range considered to include smaller values of $t$ while maintaining the same level of agreement. A cut-off parameter of $\tau = 0.8ps^{-1}$ was chosen, however it proved difficult to obtain a fit in good agreement with the experimental data of Figure 5b.

The double exponential decay is particularly prominent in the ISF for greater $\Delta K$ values depicted in Figure 6, however 'kinks' in the ISF curves at lower values of $\Delta K$ enabled consistent analysis of all curves within this experimental range. These features tend to be characteristic of higher friction regimes, and correspond to the different scales of jump diffusion across the surface.

## 5 Conclusion

The effect of varying parameters (particularly the cut-off noise filter) on particle trajectories was discussed, and the resulting ISFs were in agreement with the analytic lineshapes. The ballistic ISF obeyed a general Gaussian fit, with $\mathbf{K}$ and $1/\sigma$ having a

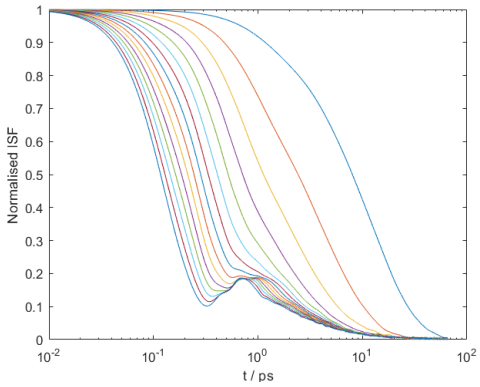


**Fig. 6** Single particle incoherent ISF, plotted over $80ps$ with sampling at $1fs$ intervals. Averaged over 1000 Li particles subject to a Cu (111) potential, over a range of $\Delta\mathbf{K}$ from $0.1 - 1.5\text{Å}^{-1}$, and at baseline parameters $m = 7amu, T = 140K, \eta = 1ps^{-1}, \tau = 0.8ps^{-1}$.

constant of proportionality given by $\sqrt{k_B T/m}$, or 4.078Å, which was in agreement with the statistical gradient of $4.058 \pm 0.03$Å.

A potential energy surface was introduced to allow comparison to experimental data; in this report Li diffusion on a Cu (111) surface is considered, allowing observation of the characteristic jump diffusion motion typical in a corrugated potential surface. A noise filter is also utilised to better replicate the physical noise spectrum, and allows greater agreement with experimental data in Section 4.5, however a low pass filter alone is insufficient to replicate the experimental trends observed. It is suggested that more advanced filters are utilised to replicate this phonon spectrum of the metal surface more accurately, in order to achieve better agreement with the experimental data.

## References

[1] G. Alexandrowicz and A. P. Jardine, "Helium spin-echo spectroscopy: studying surface dynamics with ultra-high-energy resolution", Journal of Physics: Condensed Matter **19**, 305001 (2007).

[2] A. Jardine, H. Hedgeland, G. Alexandrowicz, W. Allison, and J. Ellis, "Helium-3 spin-echo: principles and application to dynamics at surfaces", Progress in Surface Science **84**, 323–379 (2009).

[3] M. Diamant, S. Rahav, R. Ferrando, and G. Alexandrowicz, "Interpretation of surface diffusion data with langevin simulations: a quantitative assessment", Journal of Physics: Condensed Matter **27**, 125008 (2015).

[4] N. Avidor, P. Townsend, D. Ward, A. Jardine, J. Ellis, and W. Allison, "PIGLE — particles interacting in generalized langevin equation simulator", Computer Physics Communications **242**, 145–152 (2019).

[5] J. L. Vega, R. Guantes, and S. Miret-Artés, "Quasielastic and low vibrational lineshapes in atom–surface diffusion", Journal of Physics: Condensed Matter **16**, S2879–S2894 (2004).

[6] J. L. Doob, "The Brownian Movement and Stochastic Equations", Annals of Mathematics **43**, 351–369 (1942).

[7] R. Kubo, "The fluctuation-dissipation theorem", Reports on Progress in Physics **29**, 255–284 (1966).

[8] P. S. M. Townsend and D. J. Ward, "The intermediate scattering function for quasi-elastic scattering in the presence of memory friction", (2018).

[9] N. Avidor, *Na364/pigle v1.0.0-beta2*, 2018.

[10] P. S. M. Townsend and A. W. Chin, "Intermediate scattering function and quantum recoil in non-markovian quantum diffusion", Physical Review A **98**, 10.1103/physreva.98.022106 (2018).

[11] D. Ward, "A study of spin-echo lineshapes in helium atom scattering from adsorbates" (University of Cambridge, 2013).